SENSORLESS SPEED MEASUREMENT IN INDUCTION MOTOR DRIVES USING A DOUBLE ALGORITHM APPROACH

A thesis submitted to the Institute of Information Sciences and Technology, Massey University, in partial fulfillment of the requirements for the degree of

Master of Technology
in
Information Sciences and Technology

William Stanley Phipps

2002

ABSTRACT

Sensorless speed control in induction motor drives is a new emerging field offering many benefits over traditional methods. The thesis examines a method of improving the performance of sensorless speed control systems using a double algorithm approach. The rotor slot harmonics are used to determine the speed of an induction motor. This is possible as the rotor slots produce slot harmonics in the airgap field, which modulate the stator flux linkage at a frequency proportional to the rotor speed. This method, however, has limitations, at low revolutions the harmonics cannot be detected. An empirically derived formula is used to determine the speed of rotation in the speed range where the rotor slot harmonics cannot be used. The rotor slot harmonics are located and the empirical formula determined for a given 0.33HP induction motor. The final proposed system uses both mentioned methods and is simulated to determine the theoretical performance. The speed detection algorithm using the rotor slot harmonics is also implemented, with good results.

DECLARATION

I declare that this is my own work. It is being submitted for the degree of master of technology in information engineering at Massey University. It has not been submitted before for any degree in any other university.

I would like to dedicate this thesis to the Lord, who has given me inspiration and direction throughout the project. Also to my wife, Kaaren, who has supported me all the way.

PREFACE

The research was undertaken in order to fulfill the requirements for the master of technology degree in information engineering. The research undertaken was aimed at finding methods of improving on existing sensorless speed control techniques. I wish to thank the Eastern Institute of Technology for funding the research undertaken, as well as the supervisors Ibrahim Al-Bahadly and Subhas Mukopadhyay who contributed towards the completion of the research.

CONTENTS

CHAPTER 4

EXPERIMENTAL RESULTS

CHAPTER 5

SIMULATION

CHAPTER 6

IMPLEMENTATION

CHAPTER 1

INTRODUCTION

The induction motor is the most commonly used motor to date. The reason being that it requires practically no maintenance, is robust, can work in harsh conditions and is relatively cheap. As a result much attention has been given to induction motor control methods for starting, braking, speed changing, etc.

Also, because of advances in solid state power devices and digital signal processors, variable speed drives using switching power converters are becoming increasingly popular. Switching power converters offer an easy way to regulate both the frequency and magnitude of the voltage and current applied to a motor. As a result, much higher efficiency and performance can be achieved by motor drives with less generated noise.

The traditional method of closed loop motor control has been to use one or more sensors to provide feedback. A growing number of applications are now eliminating the sensor through one of several methods, such as back electromotive force (EMF) or inductance measurement, etc.

The traditional method of motor control has several disadvantages:

1. In the low power range of drives the price of a speed sensor may be more than the motor itself.
2. In some applications there is no space for them.
3. Additional wiring is required, which can be prohibitive in applications such as hermetically sealed compressors.
4. The wiring can also be vulnerable to electromagnetic interference.

Sensorless motors are best suited for applications where speed control is needed, but precise position control isn't needed. Typical applications include velocity control on conveyors, elevators, some pick-and-place applications, overhead gantries, appliance motors and centrifuges.

One type of sensorless control method involves using the rotor slot harmonics of an induction motor. When the rotor rotates the harmonics are produced in the airgap flux that induces slot harmonic voltages in the stator windings. Once the rotor slot harmonics have been detected, the speed can be easily calculated. For example, if the rotor has 44 slots the upper slot harmonic produces a frequency of 46Hz per revolution, and the lower slot harmonic produces a frequency of 42Hz per revolution. It will be shown how one of the two harmonics is isolated and the speed calculated.

Existing slot harmonic methods involve connecting an induction motor in star and summing up the phase voltages using step down transformers, this eliminates the fundamental and all even harmonics. Filtering then takes place to extract the rotor slot harmonic. A fast fourier transform technique is another method used to extract harmonic information, however, the algorithms used are fairly complex. At lower speeds, however, speed estimation becomes difficult as low frequency ripple occurs, due to the slow rotation of the rotor slots. This results in a distorted feedback signal. Methods involving signal injection are used to overcome this disadvantage, however, these techniques involve extensive off-line testing and require additional hardware.

A method of improving the performance of a system using the rotor slot harmonic technique is investigated. This involves the use of an empirical formula to estimate the rotor speed, based on current and frequency readings. This is used in the low speed range where the rotor slot harmonics become difficult to detect. Also, an improved method of rotor slot harmonic detection is tried and tested.

The proposed method is relatively easy to implement as it has few hardware requirements, and the software algorithm is simple as well. The new system will improve on the existing rotor harmonic technique of speed estimation by making the system more robust. The traditional weaknesses of the rotor slot harmonic technique is overcome by the introduction of an empirical formula to produce low speed estimation. This has the potential to improve on existing induction motor control, by increasing the dynamic speed range of a system that uses rotor slot harmonic speed estimation, in a direct field orientated control system.

CHAPTER 2

SIGNIFICANT PRIOR RESEARCH

2. SPEED ESTIMATION METHODS INVESTIGATED

In order to develop a reliable system of sensorless control, an accurate model of the system is needed, in particular accurate speed estimation. Various methods of sensorless speed control were investigated; they include:

- Speed estimation based on machine harmonics.
- Spectral analyses.
- Signal injection techniques.
- Model reference adaptive systems.
- Observer based systems.
- Kalman filter.
- Neural network based speed identification.

2.1 SPEED MEASUREMENT USING MACHINE HARMONICS

In an induction motor there are slots on the surface of the stator and rotor iron cores. When the rotor rotates, harmonics are produced in the airgap flux that induces slot harmonic voltages in the stator windings. By measuring either the magnitude or frequency of the slot harmonics the rotor speed can be determined. In [1] an early attempt at using rotor slot harmonics is undertaken. The motor is connected in star and the phase voltages summed up as shown in figure 2.1.

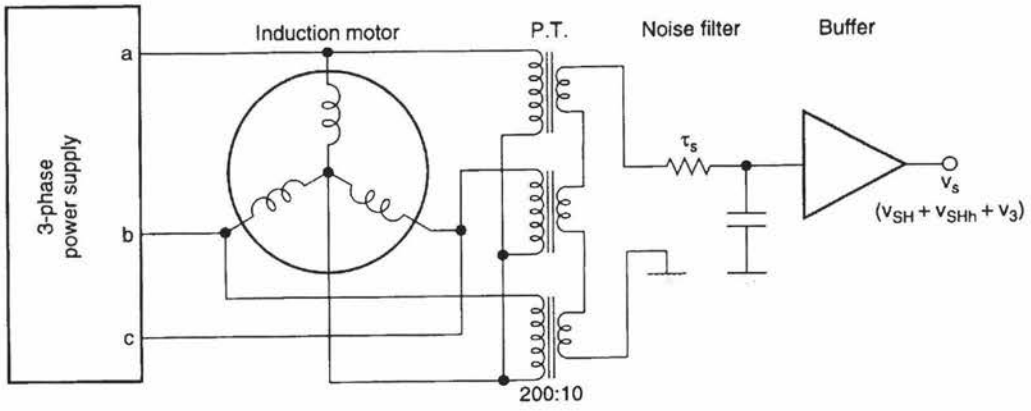

Figure 2.1 Rotor Slot Harmonic Detection Circuit (Ishida (84), pp. 577)

This results in the fundamental harmonic as well as all even order harmonics canceling out. Also, the summing results in only one of the two slot harmonics remaining with others that are a multiple of three times the fundamental. The rotor slot harmonic is sensed from the voltages induced in the coils in two of the three motor phases. The voltages are accessed by making available tapped stator winding connections as in figure 2.2. The figure shows the coil placement and taps on one phase of a double layer lap winding having a 7/9 slot pitch.

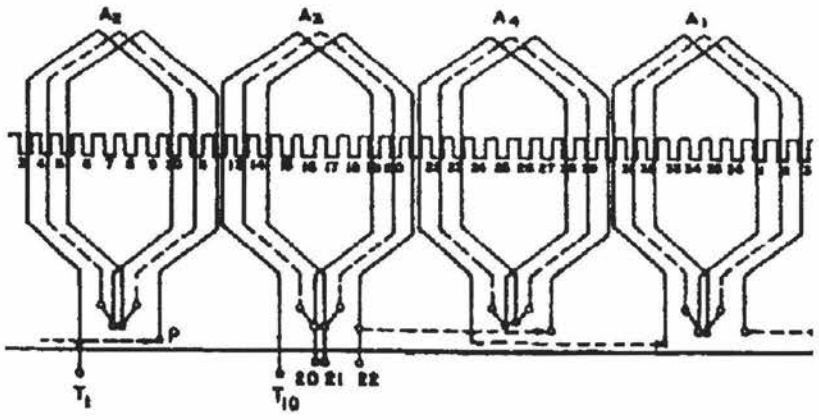

Figure 2.2 Tapped Stator Windings (Zinger (90), pp. 447)

The frequency of the rotor slot harmonic is isolated by using an analogue phase locked loop. A switched capacitor filter is also used, to allow easy filtering of the rotor slot harmonic frequency. The system is controlled by a 286 microprocessor.

Using analog devices has some disadvantages, the first being that extra hardware is needed for the application, which adds to the cost of the system. Factors, such as time constants and variations by temperature, become important. The phase locked loop requires careful choice of parameters, such as lock-in-frequency and capture frequency for correct operation. The need for tapped stator windings limits the application from using general off-the-shelf induction motors as special construction is needed to make the stator access points available.

The results showed good speed control at higher speeds with regulation deteriorating at lower speeds; this is a common problem with using rotor slot harmonic measurements.

An improvement in the technique can be seen in [2]. The rotor slot harmonics are used to determine the speed by using the frequency of the harmonics. The rotor slot harmonic is also isolated by summing the phase voltages as in figure 2.1. A parameter adaptation scheme is used to eliminate the speed estimation error by on-line tuning of model parameters. The estimation error is caused by rotor resistance changes caused by temperature, the changes in stator inductance, caused by changes of magnetization and the variation of leakage inductance due to saturation of stator teeth. The harmonics are located by using a digital bandpass filter, the centre frequency is tuned to the harmonic frequency. This offers an improvement as all the filtering can be done on the digital signal processor (DSP), thus reducing the analogue hardware needed.

Improving the speed estimation error is done by comparing the rotor harmonic frequency to the estimated rotor frequency, based on the rotor resistance model. This results in a signal, which can be used for direct feedback with enough accuracy to be used in high performance drives.

Speed errors were reduced to 0.2% and fast dynamic response was observed. This system however, was only tested using speed reversals from -4500rpm to +4500rpm and was not tested at sustained low speed.

In [3] a method was used to detect the slip frequency using the rotor slot harmonics. The rotor slot harmonic voltage is obtained by summing the three phase voltages, and after being sampled with a multiple of the stator frequency, it is changed into slip frequency waves, from which a voltage proportional to the slip frequency is obtained.

The results showed that the slip frequency detector had good linearity in the range of frequency of about -50% to +30% of the stator frequency.

In [4] another method that is used to detect the rotor harmonics is to measure between the star point of the motor and an artificial star point of a 3-resistor network. This would provide a good suppression of all three phase signals and therefore enhance the rotor slot harmonics. A bandpass filter is then used to extract the dominant rotor slot harmonic, which is then converted into pulses using a comparator. A counter counts the pulses which relate to the speed of the motor. The block diagram can be seen in figure 2.3.

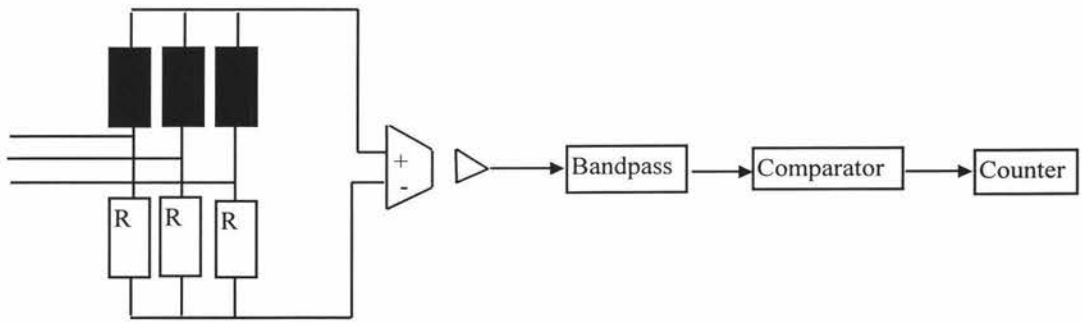

Figure 2.3 Rotor Slot Harmonic Detection Circuit (Hammerli (87), pp. 603)

The rotor speed is detected in the range 20% to 100% of nominal speed directly by the rotor slot harmonics, and in the range from 2% to 30% of nominal speed, an additional 1kHz three phase signal is fed from an inverter into the machine to produce an additional rotor slot modulation, which is used to detect rotor speed in this range.

The detector worked well in the range 2% to 100% of nominal speed range. Nonlinearities and saturation of the motor due to the PWM used, limited the detection of harmonics for very small speeds.

In [5] a method of speed measurement is used that utilises the rotor slot harmonics in combination with a Kalman filter. An adjustable digital filter is used to extract the rotor harmonics and the Kalman filter is used to estimate the harmonic frequency.

Although the results are good the algorithm is quite complex requiring amplitude, phase and frequency to be estimated in real time.

2.2 SPECTRAL ANALYSES

A method known as spectral analyses can be used at low speed [6]. Speed related harmonics from the rotor slotting and eccentricities are used to determine the speed. Since current harmonics are sampled and exist at any non-zero speed, the rotor speed can be determined at very low frequencies. The algorithm uses current harmonics, which are independent of motor parameters, and magnitude independent of source frequency. This algorithm makes up for the rotor slot harmonic's failure at low speed. However the algorithm is more computationally intensive combining several filtering steps and fast fourier transform.

Due to the discrete nature of the speed detector the system must be in steady state for a minimum period, required by the algorithm. Thus, applications like fans, pumps and conveyors are recommended.

2.3 SIGNAL INJECTION TECHNIQUES

Another method of speed estimation is to use the machine saliencies. A common approach to detect rotor saliencies is, by injecting a high frequency signal (250-1000Hz) onto the stator voltages. Using standard techniques known from signal processing, the rotor position can be extracted from the modulated stator signals. This method only works reliably for reduced flux and low loads. In high loads or flux levels, saturation in the machine causes additional modulation. This modulation cannot be distinguished from the "position harmonics" and can even cross in the spectrum. This results in a loss of control. In [7] a method termed space modulation profiling is used, which combats the deteriorating effect of saturation-induced saliencies at full flux and higher

loads by decoupling the position harmonics as a solution to enhance the position estimation accuracy. This method also reduces the unwanted modulation of the high frequency voltage at the instance of a fundamental current crossing through zero due to inverter deadtime. This allows sensorless position control under high load and full flux conditions. Since standard motors do not exhibit saliency, signal injection is always required.

A similar approach is found in [8] where high frequency signal injection is used to find the rotor flux angle. A fluctuating signal is injected into the motor and the difference in the impedance between the flux axis and the quadrature axis is measured. An arbitrary axis is taken as the estimated axis. The effect of the signal is broken down into d^e_m and q^e_m axes. If the estimated d axis is between the flux axis and quadrature axis, then the measured high frequency components on the d^e_m and q^e_m axes would be different. This difference is then the error in the rotor flux angle.

This system was not susceptible to parameter variations and had good steady state performance and could work at low speed. The algorithm used, however, does not work well for closed rotor slot motors, of which most low and medium power induction motors are of that type. Also for loaded conditions the algorithm had shortcomings due to saturation. The system described would not be satisfactory as a stand alone general purpose controller, but would be useful to complement a system that is weak in the low speed range.

2.4 MODEL REFERENCE ADAPTIVE SYSTEMS (MRAS)

With this technique a comparison is made between the outputs of two estimators. The estimator that does not involve the quantity to be estimated is considered as the reference model of the induction motor. The other estimator, that involves the quantity to be estimated, is regarded as the adjustable model. The error between the estimated quantities obtained is used to derive a suitable adaptation mechanism that generates the estimated rotor speed.

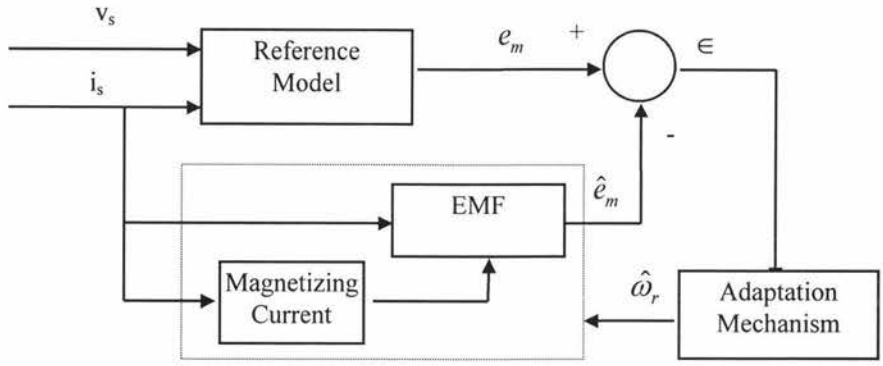

Figure 2.4 A Generic MRAS System for Speed Estimation (Peng ((94), pp. 1234)

In [9] a mutual MRAS scheme is proposed containing two models (the reference and the adjustable), which are interchangeable, allowing for rotor speed estimation and stator resistance identification. Pure integration and stator inductance are removed from the speed estimation algorithm allowing a wider speed estimation range. To eliminate the error in the estimated speed and stator resistance, on-line rotor time constant identification takes place.

Results showed that dynamic speed tracking was very good when tested through a speed reversal of ±1200rpm.

In [10] a novel MRAS method is proposed using a state observer model with the current error feedback and rotor current model as the two models for flux estimation, because current measurements are taken the model can work at low speeds unlike a voltage dependent model.

The results show a model that is more robust than a conventional MRAS scheme, showing good speed tracking when taken through speed reversals of ± 2000rpm. The methods discussed in [9] and [10] showed improved models that didn't have the shortcomings of conventional MRAS schemes such as integrator problems, small EMF at low speed and large sensitivity to resistance variation. In addition, MRAS schemes are preferred to observer based schemes because they are easier to implement and have proven stability.

2.5 OBSERVER BASED SYSTEMS

I. Adaptive Observers

Adaptive observers work by estimating the state variables and system parameters and including an error compensator to the model that establishes the observer. These systems are immune to parameter mismatch and noise. In [11], an adaptive flux observer is used, the observer estimates both speed and rotor flux. The adaptive observer uses a mechanical model to improve the speed estimation during transients. The observer can also be extended to incorporate rotor and stator resistance estimation, which results in a very accurate model of the system. The model used can be seen in figure 2.5.

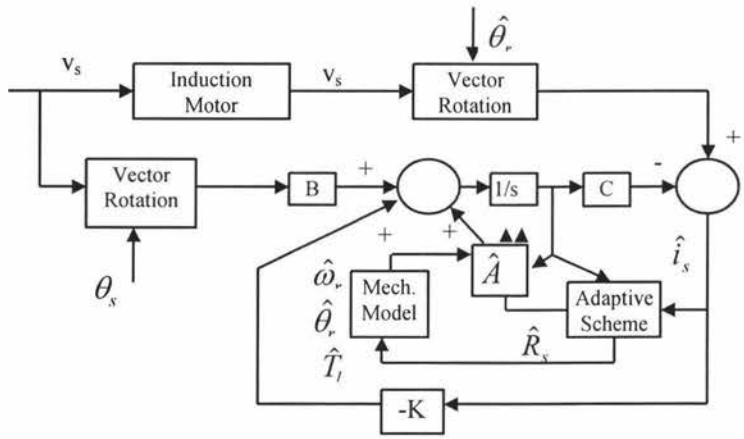

Figure 2.5 An Adaptive Flux Observer (Maes (99), pp. 2307)

The results showed good behaviour in the low speed range as well as good dynamic and steady-state-performance.

In [12] a modified observer is used which combines two models, a rotor flux orientated induction motor control and a speed adaptive flux observer. This combines the advantages of both, having the high accuracy and good torque response from the rotor flux orientated induction motor control and the good stability from the speed adaptive flux observer.

The results showed a better overall performance from the combination of the two models than just having an adaptive flux observer.

II. Sliding Observers

In [13], an adaptive sliding mode observer is used and consists of two parts, a sliding mode observer for rotor flux estimation, and a sliding mode speed identification algorithm, the two working in parallel. The sliding mode allows system tuning to take place. The observer detects the rotor flux components, namely rotor flux position ρ (needed for the field orientation), the flux amplitude ψ_r (used to close the flux control loop). The adaptive sliding mode observer operates in the two phases, stationary reference frame $\alpha\beta$. The rotor flux position and amplitude are calculated by the following $\alpha\beta$ components:

$$\psi_r = \sqrt{\psi^2_{r\alpha} + \psi^2_{r\beta}}, \qquad \rho = \arctan\left(\frac{\psi_{r\beta}}{\psi_{r\alpha}}\right)$$

An additional relation obtained by a Lyapunov function identifies the motor speed. This results in a model that is robust to parameter variations, disturbances and system noise.

Results also showed a fast convergence of the speed estimate during transients. Adaptive and sliding observers would be ideal in high performance drives where accurate flux and speed control are required. The algorithms are more complex compared to the rotor slot harmonic methods, but not as intensive as Kalman filtering methods or neural networks. The system used can be seen in figure 2.6.

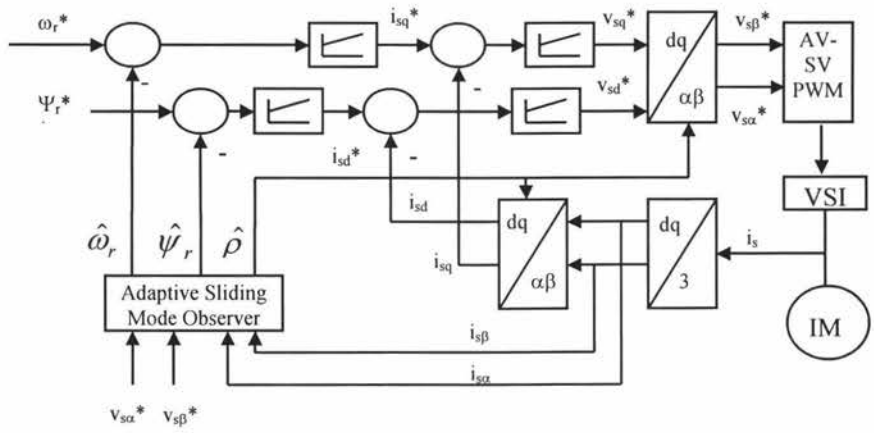

Figure 2.6 Sensorless Induction Motor with Adaptive Sliding Mode Observer (Parasiliti (99), pp. 2277)

2.6 KALMAN FILTER

The Kalman filter is used to identify the speed of the induction motor and the rotor flux, based on the measured quantities such as stator current and d.c. link voltage. Kalman filtering techniques are based on complete mathematical modeling of the induction motor. It requires the model of the a.c. motor to be calculated in real time.

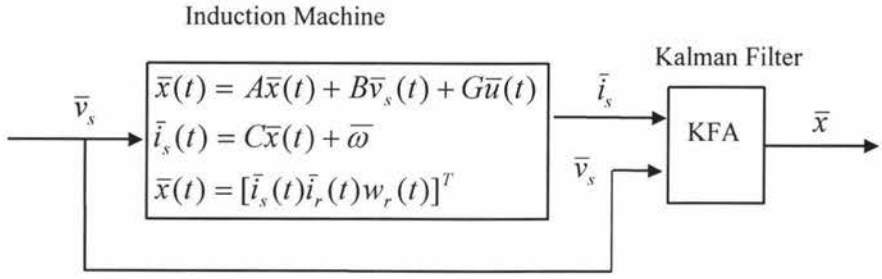

Figure 2.7 A Basic Kalman Filter Algorithm (Ilas (94), pp. 1579)

It can be seen in [14] a similar approach used, however, this time a reduced order model of the induction machine is used to reduce the computational complexity.

The results showed at 30rpm a speed error of 2rpm was obtained. A DSP32C RISC processor was used. This is a high powered 32 bit processor, which is needed to run the Kalman model showing the complexity of using this method of control. It had the best noise immunity of all the models but had poor speed estimation at sustained low speeds around 20rpm. However, the algorithm exhibits no instability at those speeds.

2.7 NEURAL NETWORK BASED SPEED ESTIMATION

The neural network technique is based on a learning process. Neural networks have the advantages of extremely fast parallel computation and fault tolerance characteristics due to distributed network intelligence. Many neurons or processing elements are interconnected to form a parallel-computing network. The most commonly used networks are the feedforward multilayer type, where no information is fed back during the training process. Feedback signals are used only during training the neural network. Generally, the back propagation method is used for adjusting the neural network

weights during the training. This is a slow and very time consuming process, as the algorithm takes a long time to converge.

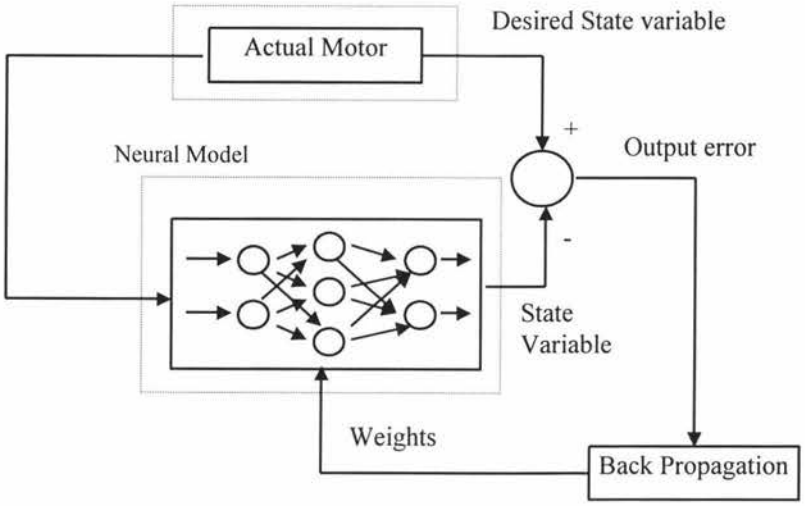

Figure 2.8 Speed Identification Via a Neural Network (Ben-Brahim (93), pp.689)

The neural network estimator has the advantage of faster execution speed, harmonic ripple immunity, and fault tolerance characteristics when compared to a DSP based estimator. In [15], the proposed neural network based speed filter uses only actual machine currents and voltages, hence the model is not dependent on machine parameters, which may not be known to the user.

Results showed that this model worked well even for fast changing loads. Neural networks however, are still an expensive and complex solution.

2.8 CONCLUSION

There is a trade off with the various sensorless systems. The ones that are easy to implement and require less complex computations tend to have poor dynamic tracking and speed estimation at low speed. This can be seen in systems based on rotor slot harmonics and, to some extent, the spectral analyses methods.

The signal injection systems tend to be cumbersome, requiring big order models with some methods producing results that would limit their usage.

The more complex type of systems using observers and Kalman filers and neural networks has a better all round performance, but at a higher cost and algorithm complexity. The better types of sensorless control methods were the MRAS schemes. The newer algorithms do not have the traditional shortcomings of MRAS controllers. Also their inherent stability and their ease of implementation make them the better choice over the observer based methods.

The Kalman filter model was the best one for speed estimation at sustained low speeds. However it's a highly complex system to implement.

The neural network approach is the latest type of sensorless control system. It had the best performance for fast changing loads, but was also the most complex model to implement.

A technique of speed estimation where there were relatively few hardware costs and which also incorporates a simple control algorithm was sought to be used in applications that didn't a require very high dynamic response, applications such as conveyors, fans, pumps, centrifuges, HVAC etc. It was found that many of the techniques already discussed required extensive algorithms and were difficult to implement requiring a fair amount of hardware as well. Sensorless speed estimation based on rotor slot harmonics matched the mentioned criteria. This technique yielded high speed accuracy in the steady state according to Jiang and Holtz [2]. However, this particular method also had the disadvantage in that at low rotor velocities, the rotor slot signals deteriorate and speed estimation was difficult. Thus, a method of extending the speed detection range was proposed by incorporating an empirical formula to work alongside the rotor slot harmonic method of speed measurement.

CHAPTER 3

RESEARCH METHODOLOGY

3. SUMMARY

A method of determining the frequency of the rotor slot harmonics and relating them to the speed of the motor needs is done by using accurate measurements of the harmonics generated. The harmonic measurements are taken using a spectrum analyser. This will determine what harmonics are present in the motor at different speeds. To determine the motor's characteristics at low speed (0-300rpm), the speed of the motor in relation to the current drawn, and the frequency, need to be obtained. The speed is measured by a tachometer attached to the motor, while the other quantities (current and frequency) are obtained directly from the display on the drive.

3.1 INTRODUCTION

The aim of the project is to investigate methods of improving on existing speed estimation techniques used for sensorless induction motor applications. A system is proposed that uses two different methods to determine the rotor velocity, the first being a rotor slot harmonic technique, this first method involves extracting the rotor slot harmonics, the frequency of which is directly related to the motor speed. The second method involves an empirical formula using current and frequency to calculate speed values. This second method involves taking the necessary readings for different loads and establishing a table of values. The current and frequency measurements are easily read off the drive and the shaft speed is accurately determined by reading an LCD display connected to a tachometer mounted on the shaft.

The first method relies on the identification of rotor slot harmonics that will then need to be isolated from the speed independent harmonics and used to determine the rotor speed.

A spectrum of the harmonics needs to be taken at various speeds in order to identify and track the rotor slot harmonics and eventually develop a "spectrum model" of the system. The final system combining both methods will be modeled using Simulink to determine its theoretical performance.

3.2 ROTOR SLOT HARMONIC THEORY

According to Nandi and Toliyat [16] the presence of rotor slot harmonics (also called principle slot harmonics or PSH) and other eccentricity related harmonics are given by the formula

$$PSH = f[(kR \pm n_d)\frac{(1-s)}{p} \pm v] \qquad (3.1)$$

where n_d=0 in the case of static eccentricity and n_d=1 in the case of dynamic eccentricity (n_d is known as eccentricity order), f is the fundamental supply frequency, R is the number of rotor slots, s is the slip, p is the number of fundamental pole pairs, k is any positive integer, and v is the order of the stator time harmonics that are present in the power supply driving the motor (v=±1, ±3, ±5 etc). However, the harmonics described in (3.1) are not present in the machine for all combinations of p and R. This is due to the fact that the only flux, which can produce voltage in a three phase stator winding, is one that has a number of pole pairs that the winding itself may produce. However, in a squirrel cage, a flux with any number of pole pairs can induce a voltage. For a machine to produce a spectrum of principle slot harmonics, the pole pair number R±np (n the harmonic order number) should be equal to the pole pair number of the space harmonics produced by a phase of the stator winding. For example, with 36 stator slots and full pitch three phase concentric winding with R=44, and p=2 the principle slot harmonics can be seen. The same winding with R=43 or 42 should not give any principle slot harmonics. The speed detection algorithms using principle slot harmonics are likely to fail for R=43 and R=42.

The PSH components are determined by (3.1) with n_d=0, v=1 and k=1, thus the PSH components are given by

$$PSH = [R\frac{(1-s)}{p} \pm 1]f \qquad (3.2)$$

Thus, in order to observe the PSH, R has to satisfy the formula

$$R=2p[3(m\pm q)\pm r] \qquad (3.3)$$

with m±q=0,1,2,3,…n and r=0 or 1.

The induction motor that is to be used for the laboratory testing has 44 rotor slots and 2 pole pairs, thus it satisfies the above formula criteria for observation of principle slot harmonics. Equation 3.2 holds as long as there are symmetric 3 phase windings, as well as for all slot types i.e. open slot, closed slot etc.

3.3 EQUIPMENT AND PROCEDURES

The spectrum analyser used was a Tektronix TDS220 digital real-time oscilloscope with a TDS2MM fast fourier transform extension module. The extension module provides FFT and a GPIB extension to interface to a variety of printers via a Centronix-type parallel port or RS232. It has the ability to print in portrait or landscape layout and supports Epson, Thinkjet, Deskjet as well as Laserjet type printers.

The FFT features include 2048 sample points, a hanning, rectangle or flat top window output display. It also has automatic measurements of rise/fall time, positive/negative pulse width and includes a 2x, 5x and 10x zoom function. The TDS220 is a 100Mhz oscilloscope with a sample rate of 1 GS/s on each of the two channels. Additional software is available to facilitate control and data logging from a P.C.

3.4 OSCILLOSCOPE MEASUREMENTS

The oscilloscope was used to measure the frequencies of the incoming signal from the induction motor. The rotor slot harmonics could then be observed and their frequency magnitude measured by using the build in features of the oscilloscope.
The accuracy of the frequency measurements are ±5Hz, measurements were taken at resolutions of either 10db and 125Hz at 2.5kS/s, or 10db and 250Hz at 5kS/s.

3.5 EXPERIMENTAL METHODOLOGY

3.5.1 EMPIRICAL FORMULA

The first set of results that are obtained are those that are needed for deriving the empirical formula to be used for open loop control. The motor is connected in a star configuration, and a 3 phase drive is used to power the motor through various speed increments. The respective readings of current and frequency are to be taken off the drive's display. The frequency and current readings are taken from 500rpm decreasing at regular intervals. Although 300rpm is deemed the cutoff point for rotor slot harmonic detection, taking readings at 500rpm would help provide sufficient data for statistical analyses when deriving the empirical formula for the motor.

The motor being tested had the following specifications:

HP 0.33
Volts 400/230 (Star/Delta)
Amps 0.9
RPM 1500

The drive had the following specifications:

Input 220V-240V 50Hz-60Hz 2.2kVA
Output 20-230V 0-240Hz 0.75kW

The speed is to be initially set at 500rpm and the load increased from no load up to full load in regular increments using the scheme in figure 3.5.

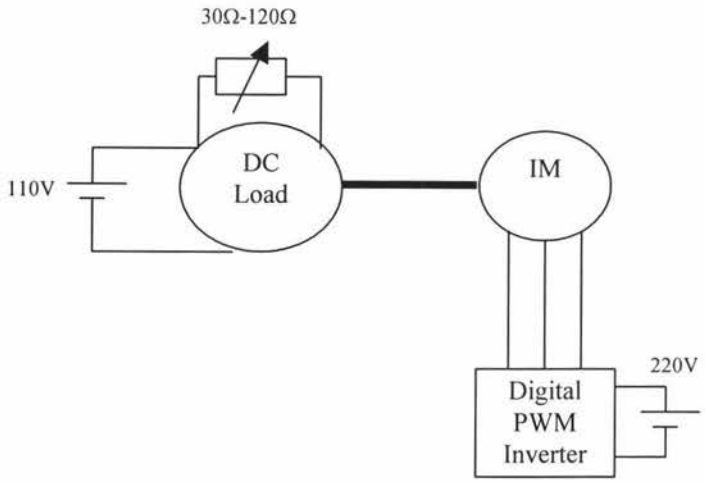

Figure 3.5 Scheme for Empirical Formula Data Collection

By varying the rotor resistance of the d.c. load attached to the induction motor, the stator of which has 110V rated d.c. voltage applied to it, the load on the induction motor can be varied. The resistance is set so that rated current of 0.9A will be drawn by the induction motor, which indicates full load. The load is decreased in regular increments down to zero load. At each load the speed is decreased in increments of 50rpm from 500rpm to 0rpm using the drive's speed control, and the frequency and current is measured from the drive's display. Once the readings are collected, statistical analyses is to be performed to determine if there is a linear relationship between the variables of current and frequency. Minitab 13 will be used to determine this by linear regressional analyses. Linear regression is chosen as the preferred statistical analyses as it is well known and can be observed that the speed is linearly related to the frequency and current fed from the drive.

3.5.2 HARMONIC ISOLATION METHOD

The scheme that will be used is the same as in figure 3.5 except no drive is used, as it will introduce its own harmonics making detection difficult. A 3 phase test sinusoidal signal is injected into the motor. This is to be done by connecting a 3 phase transformer that steps down from 440V to 110V, and feeding the 110V signal into the star

connected motor. This voltage will be enough to generate a torque and induce the rotor slot harmonics. The measurement will be taken across one phase with a spectrum analyser and the resulting waveforms identified. According to equation 3.2 there are two principle slot harmonics, which can be expected, and they are related by the number of rotor slots, the pole pair, the supply frequency and the slip. The number of rotor slots is 44 and there are 2 pole pairs. Also the supply frequency is 50Hz. The only variable is the slip. The induction motor is connected to a d.c. load, so by adjusting the load on the motor, the speed will begin to differ from the synchronous speed, and the slip can be calculated. Spectrum printouts will be taken and analysed to see if the harmonic pairs are indeed located as per equation 3.2.

Once this has been established the next step will be to try and reduce the number of extraneous speed independent harmonics so as to expose the harmonic pairs by reducing the spectrum width. This will be done by using a passive bandpass filter of 1st and 2nd order, and observing the effect of both. The filter is made by combining an RC low pass filter with an RC high pass filter. The expected speed range is from 1460rpm -1100rpm, which corresponds to 1022Hz –770Hz of the rotor slot frequencies. The bandpass cutoff frequency can be any value in that range. This will result in the attenuation of high and low frequency harmonics while the rotor slot frequencies have a small attenuation. The cutoff frequency was chosen to be 1kHz. The phase voltage is 64V, so a resistive voltage divider is needed to reduce the voltage before applying it to the bandpass filter built on a breadboard. The voltage is reduced to about 13V and the signal is then applied to the bandpass filter circuit.

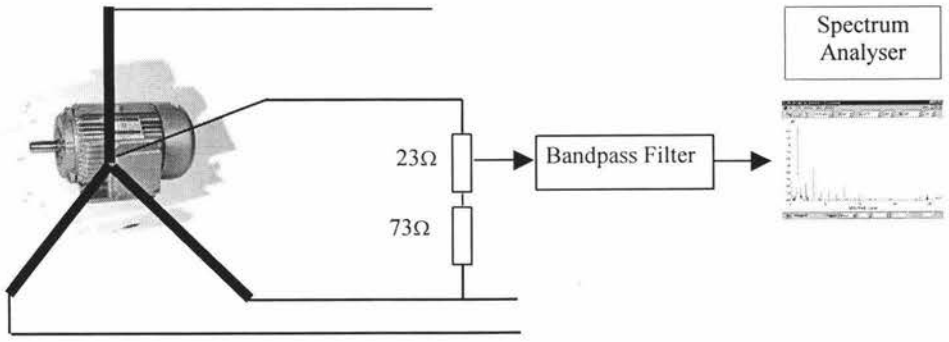

Figure 3.6 Experimental Setup

3.6 PARAMETER VARIATIONS AND ACCURACY

The estimation of the rotor slot harmonic depends on various machine parameters. These vary in a fairly wide range. During operation:

- The rotor resistance changes with the machine temperature.
- Variations of the stator inductance are caused by changes of magnetisation.
- The variation of the leakage inductance, due to saturation of the stator teeth.

The rotor frequency equation is shown below in the stator dq reference frame:

$$\omega_r = \frac{l_s i_{sq}}{\tau_r \psi_{sd} - \sigma l_s i_{sd}} \qquad (3.3)$$

where l_s is the stator inductance, i_{sq} is the torque producing current, τ_r is the rotor time constant, ψ_{sd} is the stator flux and the leakage inductance is σl_s.

Practical considerations permit the following simplifications:

- The leakage flux $\sigma l_s i_{sd}$ is only a fraction of the stator flux ψ_{sd}. Hence the term ψ_{sd}-$\sigma l_s i_{sd}$ is fairly unsensitive to leakage inductance variations.
- Since $\frac{l_s}{\tau_r} = \frac{l_s}{l_r} r_r \approx r_r$, the accuracy of the rotor frequency estimation depends primarily on the rotor resistance. Hence, equation 3.3 converts to

$$\omega_r = r_r \frac{i_{sq}}{\psi_{sd} - \sigma l_s i_{sd}} \qquad (3.4)$$

The equation shows that at a given load and magnetisation, the estimated rotor frequency ω_r is directly proportional to the rotor resistance. From this, it is expected that the more the motor is loaded the more the rotor slot harmonic error will increase, due to the increased slip which causes an increase in the rotor resistance.

CHAPTER 4

EXPERIMENTAL RESULTS

4. EMPIRICAL RESULTS

The tables 1-8 in appendix A show the experimentally measured values, they will be used to derive the empirical formula.

The readings of current and frequency were obtained from the drive's display and shows what was been fed to the motor. The corresponding speed readings were taken off a tachometer mounted on the shaft. Each table from 1 to 8 corresponds to a different load. In table 1 there is no load applied to the motor, while table 8 shows the full load readings.

Using minitab 13, an attempt was made to see if there was a mathematical relationship between the frequency, current and speed. The voltage was not considered as part of the formula as it is always proportional to the frequency.

The following results of regressional analyses were obtained:

```
The regression equation is
speed = 287 + 8.89 freq - 969 current

Predictor        Coef     SE Coef          T        P
Constant       287.15       16.37      17.54    0.000
freq           8.8946      0.2112      42.12    0.000
current       -969.45       44.12     -21.97    0.000

S = 25.66       R-Sq = 96.9%     R-Sq(adj) = 96.8%
```

From the results we have in the first column the estimated coefficients, in the second column are their standard errors. In addition a T-value that tests whether the null hypothesis of the coefficient is equal to zero and the corresponding P-value is given. The P-value is the probability of obtaining a sample result that is more unlikely than what is observed. As can be seen the P-values are all zero, which indicates that it is highly likely that the coefficient values will hold true.
The S-value is the estimated standard deviation about the regression line. The R-value is the proportion of variability in the speed variable accounted for by the predictors (frequency and current). It determines how much the equation will deviate from its linearity. R-sq(adj) is r adjusted for degrees of freedom. If a variable is added to an equation, R will get larger even if the added variable is of no real value. To compensate for this minitab prints out the R-sq(adj). It is the approximately unbiased estimate of the population r that is calculated by the formula converted to a percent. The R-Sq(adj) value is 96.8 %, which means that there is a 96.8 % probability of a linear relationship between the variables.

4.1 SPEED EQUATION

From the result of the regressional analyses, an equation is derived

$$\text{speed} = 287 + 8.89\ \text{frequency} - 969\ \text{current}. \qquad (4.1)$$

This equation will be used to estimate the speed in the open loop region of operation. The formula produces a maximum 5% error compared to the actual rotor speed, in the range 500-120rpm. Below 100rpm, the error increases substantially as the rotor looses torque at low frequencies (See figure 4.2). These errors are due to the fact that the empirical formula is only a linear approximation over the speed range and will therefore have values that are not the exact expected values.

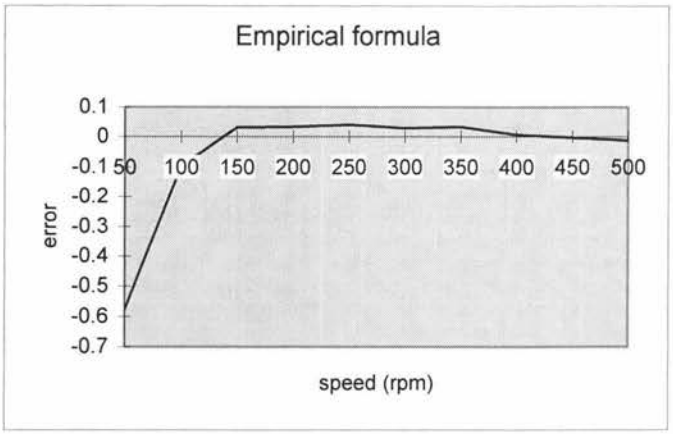

Figure 4.2 Empirical Formula Error

This error can be improved by taking note that between 400rpm and 150rpm the error is positive. By decreasing the reading that the formula produces by 3% between 400 and 150rpm, results in an improved response. Also from 150rpm down to 0rpm the speed error is negative, so by increasing the readings by 9% produced a much better result, notably that the greatest error now is only 1.1% between 500-100rpm. This calculation will be performed by the microcontroller in the final system.

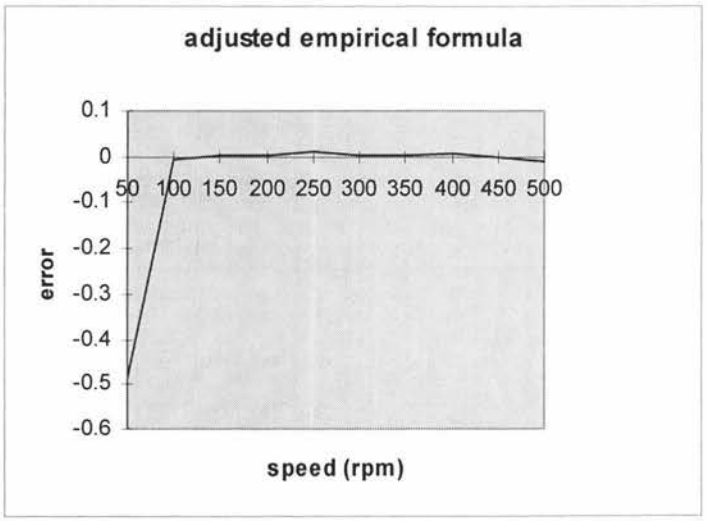

Figure 4.3 Adjusted Empirical Formula Error

4.2 ROTOR SLOT HARMONIC RESULTS

The Spectral results were obtained at different speeds by applying a 50Hz 3 phase 110V signal into the stator of the motor, and by increasing the load on the motor by means of a d.c. brake. That way the slip was varied and the resultant harmonics recorded using a spectrum analyser. The rotor slot harmonic's position was calculated by using the following formula:

$$PSH=[N_r(1-s)\pm1]f \qquad (4.2)$$

Where N_r = number of rotor slots per pole pair

s = slip

f = frequency

The motor was taken through 4 different speeds and the harmonic frequency components were analysed. Table 9 shows the expected harmonic frequency values.

Table 9 Speed vs Rotor Harmonic Frequencies

Speed rpm	Upper Harmonic Hz	Lower Harmonic Hz
1460	1121	1021
1400	1077	977
1320	1018	918
1100	857	757

The spectrum was analysed to determine if the rotor slot harmonic pairs were indeed where they were theoretically supposed to be. The results can be seen in appendix B figures 1 to 4. The cursor 1 and cursor 2 readings relate to the frequency measurement of the vertical lines. Looking at table 9, one can see that the theoretical frequencies of the harmonics appear to relate to the measured ones, taking into consideration that the resolution of the spectrum analyser is only ±5Hz.

The next step was to apply the phase voltage to the bandpass filter and observe the resultant spectrum (see figure 3.6). The signal was applied to a 1st order and then a 2nd order bandpass filter to compare the outputs. The resultant spectrums can be seen in appendix B figures 5 to 12.

The results show that only one of the two rotor slot harmonics remains after filtering. The lower order harmonic is the one that remains, while the higher order harmonic disappears (see table 9). As can be seen from the figures, cursor 1 shows the frequency of the harmonic, while cursor 2 is placed on the fundamental so the relative magnitudes can be observed. It can be seen that as the load is increased and the speed decreases, the rotor slot harmonic increases in magnitude. For a speed of 1100rpm, taken through the 1st order filter, the rotor slot harmonic was 39.6db, while at 1450rpm, taken through the same filter, the magnitude was 29db. This is due to the fact that as the load increases more rotor current is drawn and this, in turn, increases the harmonic magnitude. It can also be observed that the only significant speed independent harmonics remaining are the odd harmonics from the fundamental up to the seventh harmonic. These could probably be reduced with additional filtering, however the third harmonic is difficult to get rid of due to machine saturation.

In addition, the rotor harmonic signal can be amplified by taking it through an active bandpass filter if need be.

4.3 LOW SPEED ROTOR HARMONICS

It can be seen from apppendix B figure 13 that at 335Hz about 500rpm the rotor slot harmonic is in the region of the 7th harmonic. It becomes difficult for the phase locked loop to lock onto the rotor harmonic from this point downwards. This is due to the fact that there are other lower order harmonics in close proximity to the rotor harmonic. Also, the rotor harmonic magnitude reduces to that of the surrounding harmonics as the speed decreases, due to the slow rotation of the rotor slots and decreasing induction taking place (see figures 14 and 15).

4.4 SPEED CALCULATION

The rotor speed can now be easily calculated by the fact that the motor has 44 rotor slots. Using the lower order harmonic offers a signal which is equivalent to that of an incremental speed sensor having a resolution of 42 counts per revolution. The upper order harmonic produces a signal equivalent to 46 counts per revolution. Since the lower harmonic is the one that remains after filtering, the frequency per revolution is taken as 42Hz. The revolutions per minute are calculated using the formula below.

$$\text{speed} = \text{rotor harmonic frequency} \times \frac{60}{42} \qquad (4.3)$$

Testing this formula out on the frequencies obtained from the spectrum analyser, it was found that there was a difference in the rotor speed when compared to the tachometer display. It was also found that this error got worse the more the load on the motor was increased. This was expected from 3.6 that the rotor harmonic frequency is related to the rotor resistance. Thus, as more load is placed on the motor, more current is drawn and the rotor resistance increases. The tachometer results were compared with the calculated results from (4.3) and the speed error worked out as seen in figure 4.19.

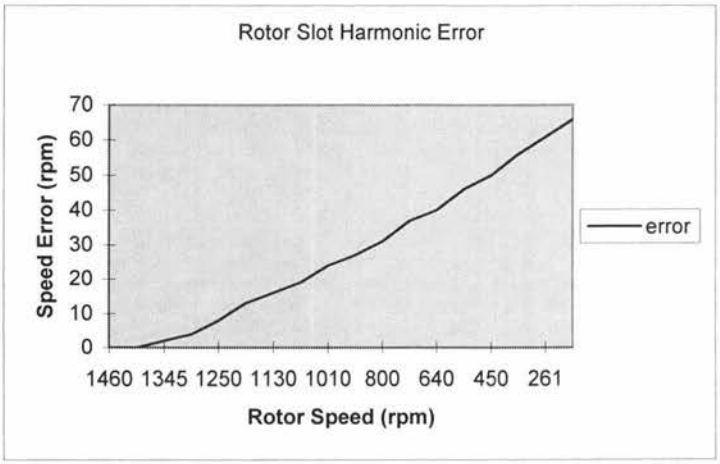

Figure 4.19 Rotor Slot Harmonic Error

The error in the rotor slot harmonic will result in an unacceptable error in the final speed calculation. A method to compensate for this will be discussed in chapter 6.

4.5 CONCLUSION

The results of the initial spectrum analyses were as expected and were consistent with previous studies. What was somewhat surprising though were the resulting readings from the output of the bandpass filter. None of the previous papers investigated used this simple approach. However, in using this somewhat simple approach, it resulted in suppression of all or most of the higher order harmonics, while leaving only the lower odd harmonics up to the seventh harmonic. The rotor slot harmonic was left exposed and nicely separated from all other spectrum components, making detection easy. The greater the number of rotor slots with respect to the pole pairs, the further out from the fundamental harmonic are the rotor harmonics.

CHAPTER 5

SIMULATION

5. INTRODUCTION

From chapter 4 it can be seen that the rotor slot harmonic can be isolated. Now a simulation of the entire speed control system is to be done. The simulation is done in Simulink 4 and is done to test the performance of the system and various parts thereof. This will help to determine if the system has any shortcomings that would need to be addressed. In chapter 6 the rotor harmonic part of the simulated system will be implemented to determine the actual performance.

5.1 HARMONIC DETECTION

A method is proposed to detect the rotor slot harmonic by locking onto it using a phase locked loop.

5.1.1 PHASE LOCKED LOOP PRINCIPLE

If an input signal is applied to the system, the phase comparator compares the phase and frequency of the input signal with the voltage controlled oscillation (VCO) frequency, and generates an error voltage Ve(t), that is related to the phase and the frequency difference between the two signals. This error voltage is then filtered, amplified and applied to the control terminal of the VCO. In this manner, the control voltage Vd(t) forces the VCO frequency to vary in a direction that reduces the frequency difference between fo and the input signal. If the input frequency fi is sufficiently close to fo, the feedback nature of the phase locked loop (PLL) causes the VCO to synchronise or lock with the incoming signal. Once in lock, the VCO frequency is identical to the input signal except that for a finite phase difference. This net phase difference is necessary to generate the corrective error voltage Vd(t) to shift the VCO frequency from its free-running value to the input signal frequency fi and thus, keep the PLL in lock.

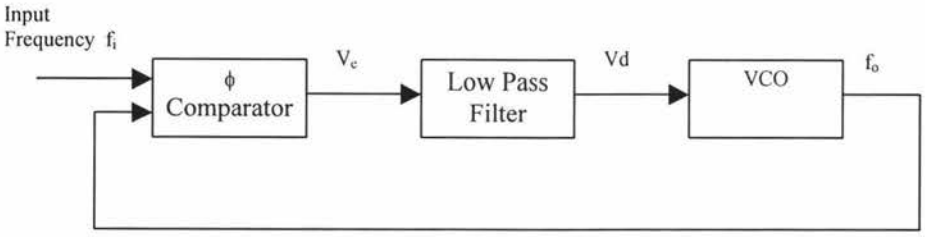

Figure 5.1 Phase Locked Loop Schematic

The range of frequencies over which the PLL can maintain lock with an input signal is defined as the "lock range" of the system. The capture range is a measure of how close the input signal's frequency must be to that of the VCO to acquire lock. The "capture range" can assume any value within the "lock range " of the system and is never greater than the "lock range", and depends primarily upon the band edge of the low pass filter together with the closed loop gain of the system. It is this signal-capturing phenomenon, which gives the loop its frequency selective properties.

5.1.2 PHASE LOCKED LOOP DESIGN

In order to design a phase locked loop two things need to be known, and that is the lock range $\Delta\omega_L$ and the capture range $\Delta\omega_C$. The lock range is equal to the loop gain which is given by $\Delta\omega_L=K_dK_o$ where K_d is the phase comparator sensitivity and is the output voltage from the phase comparator per radians of phase difference at the phase comparator. A value of 3 volt/rad was chosen, this value is externally adjustable in most PLLs. K_o is the oscillator sensitivity and is determined by the choice of timing capacitor and gain control resistor connected externally and is set to 1257 rad/sec/volt. The capture range is expressed as $\Delta\omega_C \approx \sqrt{\frac{\Delta\omega_L}{T}}$ where T is the filter time constant. It is necessary to set the capture frequency to be equal to the largest slip component, this will allow locking onto the slot harmonic, without much of a possibility of locking on another signal. A slip of 25% was chosen which translates to approximately Δf_C=300Hz.

It is necessary to set the VCO oscillation frequency in the middle of the expected maximum and minimum slot harmonic frequency per induction motor input frequency.

Since the maximum slip is 25% a midway slip would be 12.5%, so using the formula for the lower slot harmonic (LSH), LSH=$(N_r(1-s)-1)f$ and setting the slip to be 12.5% gives 18.4f. Since the rotor slot harmonic is related to the driving frequency, this will ensure that the VCO frequency of the phase locked loop is in the centre of the largest expected harmonic range. Thus, whatever the driving frequency, as the load varies from no load to a maximum load, the phase locked loop will have the capture range to lock onto the rotor slot harmonic.

Using these values and the formula $\Delta\omega_L=K_dK_o$ gives $\Delta\omega_L$=2513rad/sec or f_L=400Hz. The maximum slip dictates that $\Delta\omega_C$=1885rad/sec or Δf_c=300Hz. The filter time constant is left to be calculated, so using $\Delta\omega_C \approx \sqrt{\frac{\Delta\omega_L}{T}}$ and substituting and solving for T gives T=707.25μs. From that, the cutoff frequency of the 1st order low pass filter used in the PLL can be determined by using the well-known formula $f_{cutoff}=\frac{1}{2\Pi T}$ which gives f_{cutoff}=225Hz. These values will be used to determine the phase locked loop performance in the simulation.

5.1.3 PHASE LOCKED LOOP SIMULATION

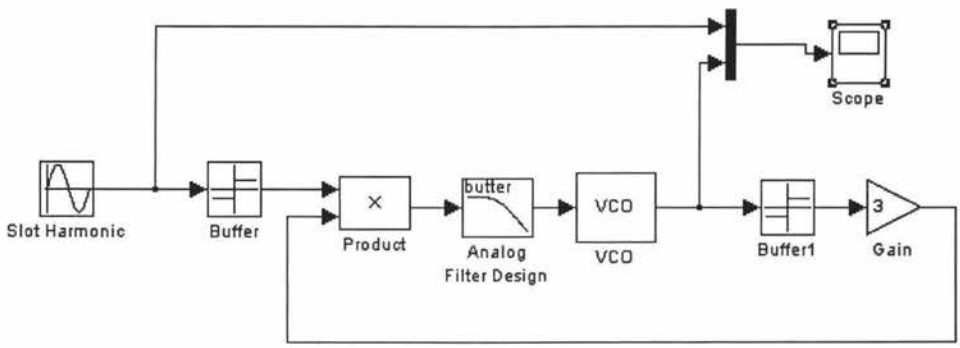

Figure 5.2 PLL Operation

Figure 5.2 shows the phase locked loop system based on the design mentioned in 5.1.2. The final PLL will have a controlled VCO so that the centre frequency of oscillation can be adjusted by a microcontroller or DSP as the motor frequency and therefore the rotor slot harmonic changes.

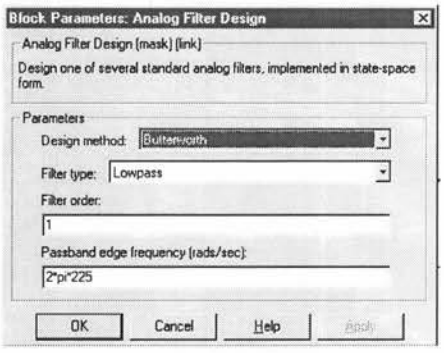

Figure 5.3 Block Parameters of Analog Filter Design

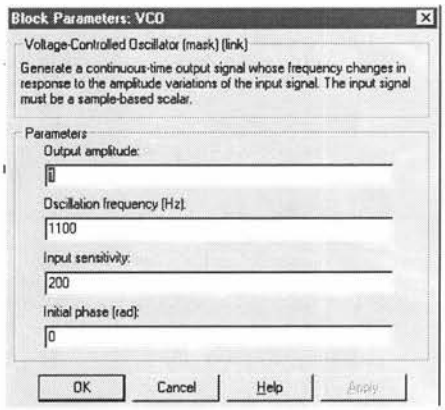

Figure 5.4 Block Parameters of VCO

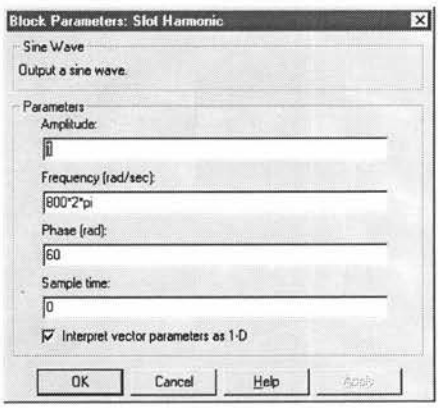

Figure 5.5 Block Parameters of Rotor Slot Wave

5.1.4 PHASE LOCKED LOOP RESULTS

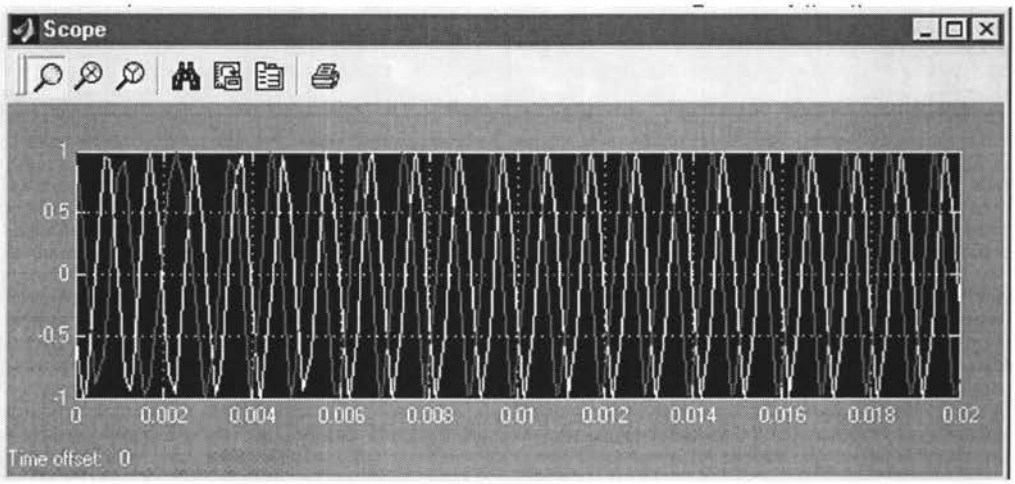

Figure 5.6 Waveforms with Input at 1000Hz and VCO 1050Hz

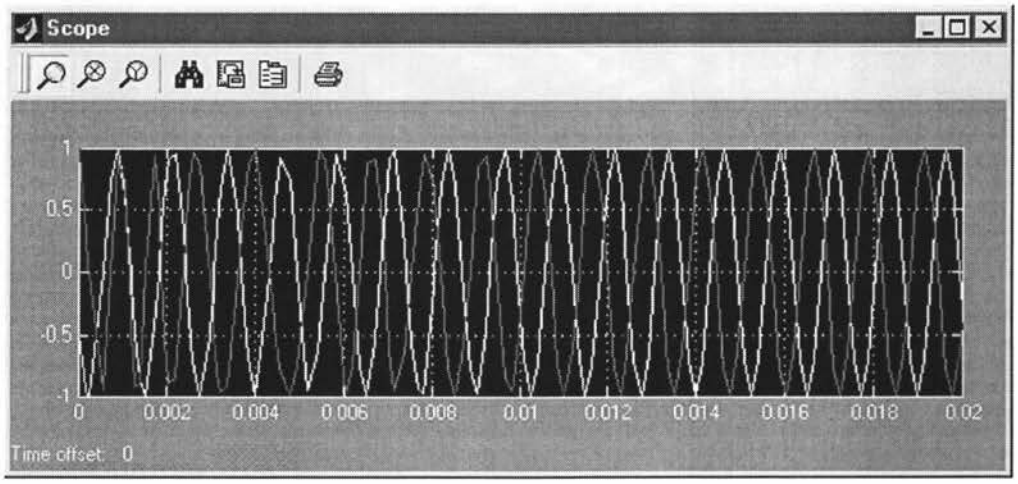

Figure 5.7 Waveforms with Input at 800Hz and VCO at 1100Hz

It can be seen from the results of 5.1.4 that the phase locked loop operates successfully within the desired capture range of 300Hz as required. It can also be seen from figure 5.6 and 5.7 that the greater the frequency difference between the input and VCO, the greater the phase shift is between input and VCO frequency, this is in line with the phase locked loop's operating principle.

5.2 SPEED ESTIMATION ALGORITHM

Once the phase locked loop has locked onto the slot harmonic, then the harmonic frequency needs to be converted into an rpm reading. The speed reading is then checked with a predefined speed of 500rpm.

The result will determine whether to extract the speed from the slot harmonics or to use the empirical formula based on current and frequency readings. Although 300rpm is deemed to be the frequency below which harmonic detection is difficult. In this particular method the PLL might have difficulty locking onto the rotor slot harmonic below 500rpm, as the rotor harmonic will cross the 7^{th} harmonic at this point, and is of similar magnitude. Therefore 500rpm is chosen as the point where the empirical formula takes over. If the PLL locks onto a rotor harmonic above 500rpm, then the empirical formula is deactivated.

Once the harmonic has been fed into the system (see figure 5.8), the frequency is determined and, from that, the revolutions per minute are calculated. The resolution of the motor corresponds to 42Hz per revolution. This is used to determine the rpm based on the frequency of the harmonic at the input. If the speed reaches 500rpm or less, a high is generated at one input of the AND gate, the other input gets a pulse every second. Thus, a high output of the AND gate will activate the empirical formula.

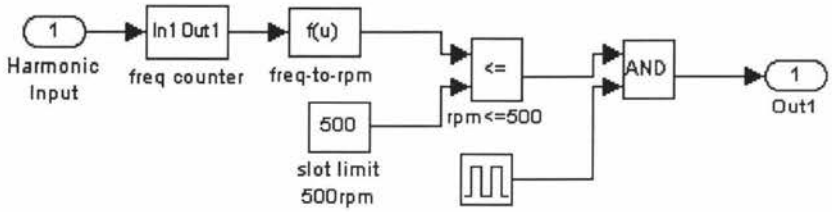

Figure 5.8 Speed Algorithm Switch

5.2.1 FREQUENCY COUNTER

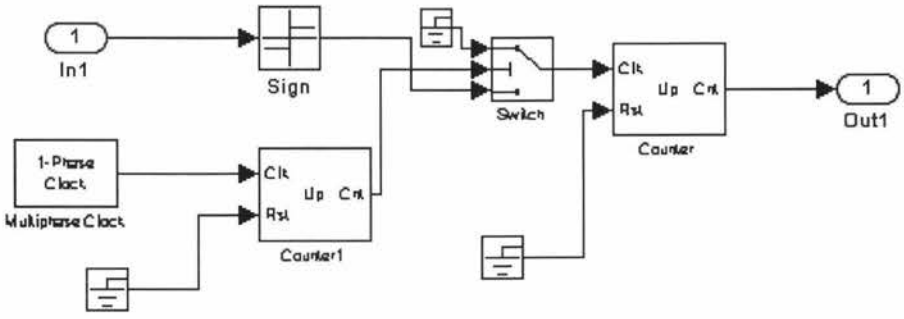

Figure 5.9 Frequency Counter Block

The frequency counter block can be seen above and works by counting the changes at the input for 1s. The multiphase clock provides a 1Hz frequency to the counter which sets the switch to sample the input for 1s.

5.3 EMPIRICAL FORMULA

The empirical formula gets implemented when the rotor speed drops to 500rpm or less, thus, it doesn't matter what harmonic the PLL locks on to below 500rpm, even if its not the rotor harmonic the formula will still be activated. When this happens, a signal is sent every second and a sample is taken of the phase current and driving frequency. These values are put into the formula that generates the expected speed output.

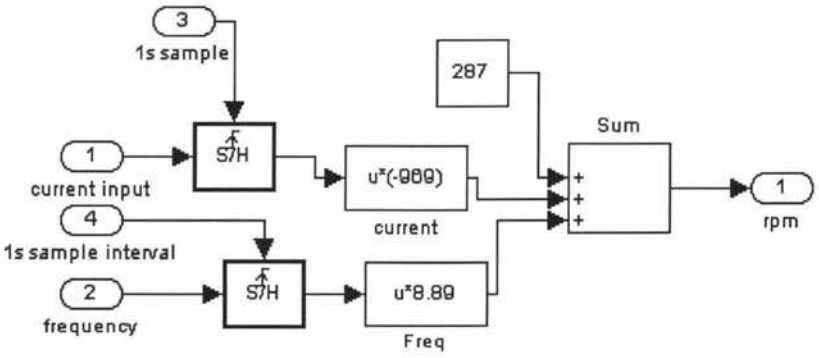

Figure 5.10 Empirical Formula Block

5.4 SYSTEM MODEL

The complete model of the system incorporating the phase locked loop and empirical formula for the speed estimation can be seen in figure 5.11.

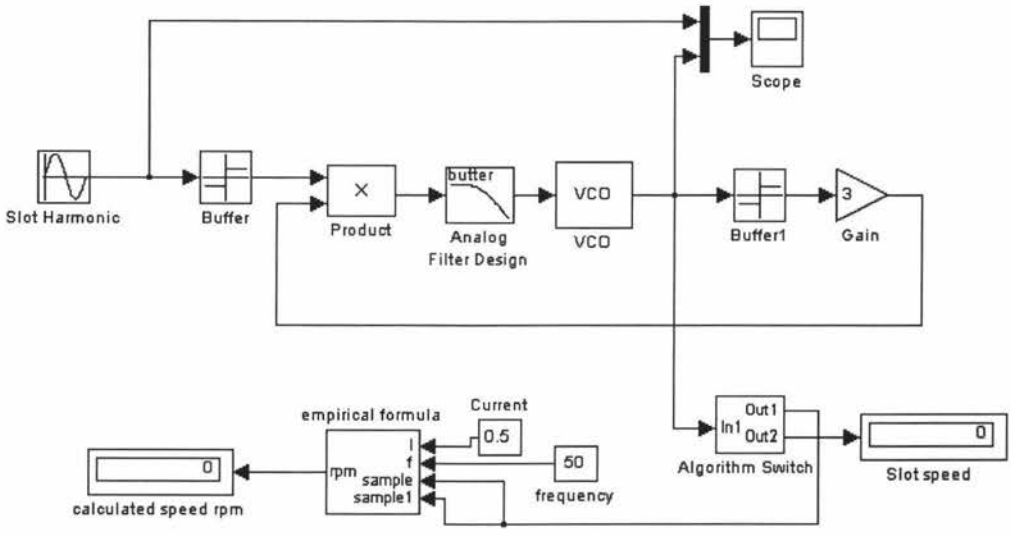

Figure 5.11 Complete System Model

5.5 CONCLUSION

The final system model performs as expected with the VCO frequency locking onto the input slot harmonic and producing speed results exactly as predicted. When the speed fell to 500rpm and below, this resulted in the empirical formula immediately taking over the speed estimation from the rotor slot harmonic, producing a speed output in accordance with the input current and frequency.

The algorithm switch shown in figure 5.8 will be a software implementation in the final system as well as using a PLL with an adjustable VCO frequency to follow the harmonic as it changes with rotor speed.

The simulation demonstrates that this type of model using two algorithms interchangeably works, and is a viable proposition in extending the range of a slot harmonic speed control system.

CHAPTER 6

IMPLEMENTATION

6. SUMMARY

The speed estimation part of the system was setup, and speed was calculated using the rotor slot harmonic, that was fed back from a phase of the motor into the bandpass filter, then into a phase locked loop (PLL) which locked onto the harmonic. The output of the PLL was then fed into a basic stamp 2 processor that measured the frequency and calculated the speed. The basic stamp code was downloaded from a P.C. via RS232 interface into the processor. A basic stamp was used because it is easy to program and just served as a "test" device for the project.

6.1 PHASE LOCKED LOOP

The phase locked loop was setup using a LM565. Using an external capacitor and resistor, the free-running frequency was set to 845Hz. Using a function generator to inject a test sine wave it was found that the capture range was 350Hz, which was close enough to the desired capture frequency of 300Hz. The exact capacitor and resistor values are difficult to come by and are also subject to tolerances. When using the PLL in the project it was found that the capture frequency was only 220Hz. This was due to the fact that the signal coming into the PLL from the bandpass filter was only 0.98V and this low input voltage affected the capture range. In the laboratory the required capture frequency of 300Hz was obtained using an 8V input sine wave from a function generator. This problem can be easily rectified in the future by feeding the signal from the bandpass filter into a common emitter type amplifier.

Having the free-running frequency set to 845Hz resulted in the actual speed range being from 1060-1380rpm.

6.2 BASIC STAMP 2

The basic stamp is a simple microcontroller consisting of a PIC16C57 chip and is programmed using a pseudo basic code. The stamp was used as it has a frequency counting instruction, and is therefore easy to program, requiring only a ground and the input from the phase locked loop. It served as a test device to check the speed operation of the system. The basic stamp has the disadvantage in that it can only do integer arithmetic, this added to the final errors between the calculated and actual speed. The final system will use a digital signal processor (DSP) to perform the calculations, so greater calculation accuracy can be expected.

6.3 RESULTS

It was found that the speed results produced by the basic stamp were significantly different from the tachometer speed-readings. This was due to the error in the rotor slot harmonic as mentioned in chapter 4. A method was derived to overcome this error and increase the accuracy. Using the rotor slot error (figure 4.19), and feeding the results into minitab 13, a formula was derived that models the slope of the error, which is highly linear. The formula derived was as follows:

$$Actual\_speed(rpm) = 70.8 + 0.95harmonic\_speed(rpm) \qquad (6.1)$$

The error between the calculated speed and the actual speed using the adjusting formula can be seen in table 6.1.

Table 6.1 Real and Calculated Speed Difference

Tachometer (rpm)	Basic Stamp (rpm)
1100	1100
1120	1120
1140	1138
1160	1158
1180	1180
1200	1198
1220	1217
1240	1237
1260	1256
1280	1276
1300	1296
1320	1317
1340	1336

6.4 HARMONIC DETECTION CIRCUIT

The harmonic detection system is seen below in figure 6.2.

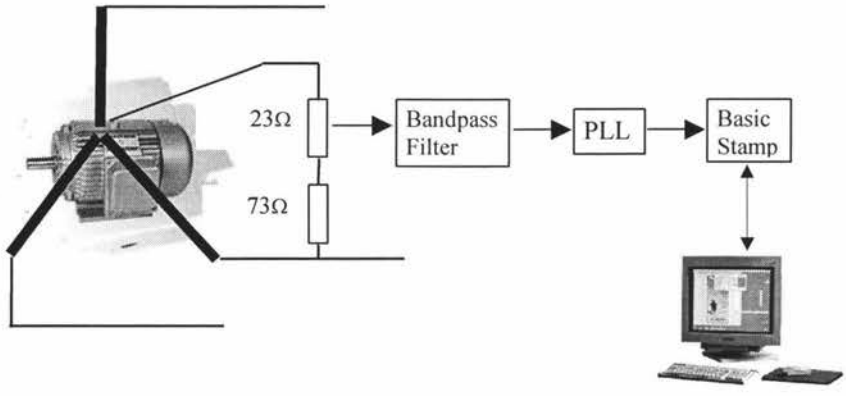

Figure 6.2 Harmonic Detection System

The harmonic detection circuit is also shown at component level in figure 6.3.

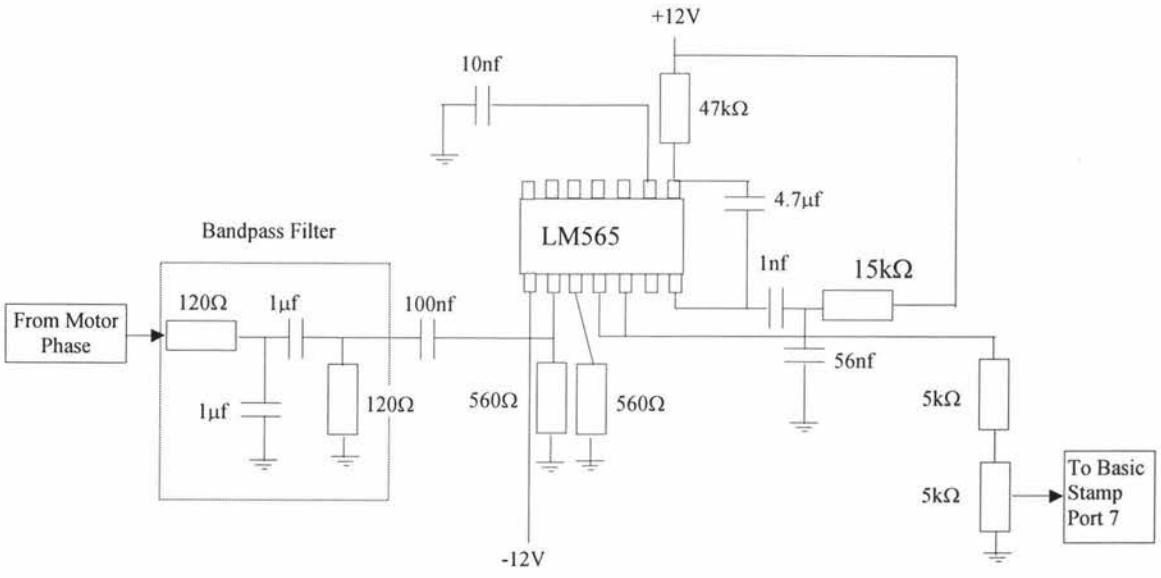

Figure 6.3 Bandpass Filter and PLL Circuit

The experimental laboratory setup can be seen below in figure 6.4.

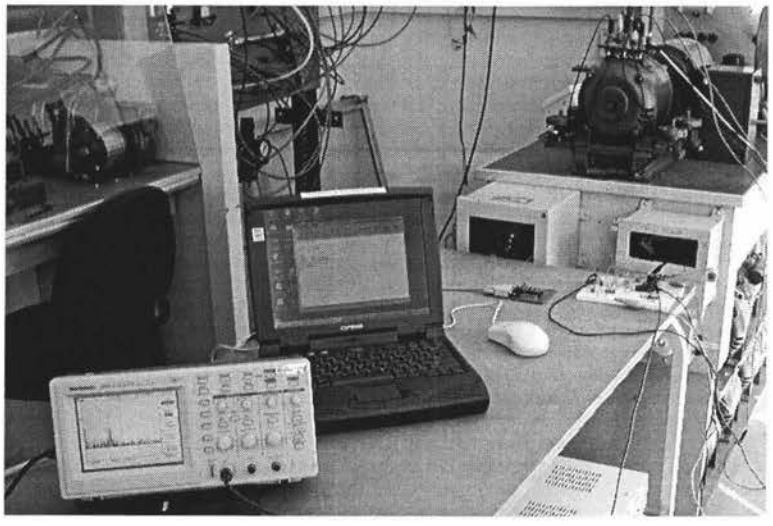

Figure 6.4 Laboratory Setup

6.5 BASIC STAMP

The frequency of the PLL was fed into port 7 of the basic stamp. The frequency was counted and converted into rpm. The rotor speed adjusting formula (6.1) was then applied to give more accurate speed estimation.

Basic stamp source code can be seen below:

```
'{$stamp bs2}

cycles var word          'declaring variable to be word length
final var word           'can hold values from 0 to 65535
variable var word        '
constant var word        '
speed var word           '

start:
count 7,1000,cycles      'counts pulses per second
final = cycles */366     'converts to rpm

variable= final*/243     'adjusting formula
constant=1*/18125        '

speed=variable+constant  'adjusted speed
debug dec speed          'show speed
goto start
end
```

6.6 CONCLUSION

The results showed that the system produces a speed estimation based on the rotor slot harmonic by locking onto the frequency of the harmonic and tracking it through a frequency range based on the phase locked loop's characteristic.

The final results using the adjusting formula for speed estimation are seen in table 6.1, and it can be seen that the maximum speed difference is no more than 4rpm between tachometer speed and calculated speed. The simulated speed results using the rotor slot harmonic closely matched the practical results when the adjusting formula was applied to compensate for the rotor error.

The final implementation will use a digital signal processor so there will be no problems with having only integer arithmetic, also a digital phase locked loop is preferred as there are no drift problems and it is easy to interface to a processor, which will be used to control the PLL's free-running frequency.

To implement the empirical formula the only external samples needed will be the current, and this can be done by using a current transformer and feeding the secondary voltage into the on board analogue-to-digital converters of the DSP. Since the PWM frequency controlling the motor will be generated from the DSP, no external sampling will be needed. The empirical formula was not implemented in the current setup as the basic stamp has no analogue to digital converters, and as well as time constraint factors prevented this from happening.

CHAPTER 7

DISCUSSION AND CONCLUSIONS

The project was developed and implemented and was shown to successfully estimate the speed of the induction motor using the rotor slot harmonic. The completed combination of the two algorithms was not done as a digital signal processor (DSP) was not available at the time. This can form the basis to develop a complete implementation later on.

The speed detection method developed involved less hardware and is simple to implement, and will provide a cheap method of controlling induction motors where high precision is not required. The empirical formula was a good way of extending the speed range of the system, as it requires no extra hardware and requires little memory to run as there are no lookup tables. The double algorithm approach is ideal for systems that don't require operating at very low speeds and provides a simple cheap method of speed control requiring minimal hardware and software. The system can run successfully from 100rpm and higher. Other systems that have been able to measure lower speeds require highly complex algorithms to operate with some of them requiring the motor itself to be adapted.

A method to extend the rotor slot harmonic range is something for further investigation. A method of maybe mirroring the rotor harmonic to a higher frequency away from the lower order harmonics where they can be easily detected is something that can be considered.

The scheme of extracting the rotor harmonic using just a passive rc bandpass filter has according to my research not been done before. This method has an advantage in that additional steps and hardware involved in the conventional extraction of the rotor harmonic, namely, the method of summing up the phase voltages then applying filtering steps, can now be done away with. Also, to further reduce the hardware requirements a digital bandpass filter can be implemented on a DSP in the future to extract the rotor harmonic.

The DSP will also control the digital phase locked loop's free-running frequency, so as to keep the changing rotor slot harmonic within the desired capture range of the phase locked loop. The final proposed implementation of the rotor slot speed algorithm in a direct field orientated control system will be similar to the system seen below in figure 7.1.

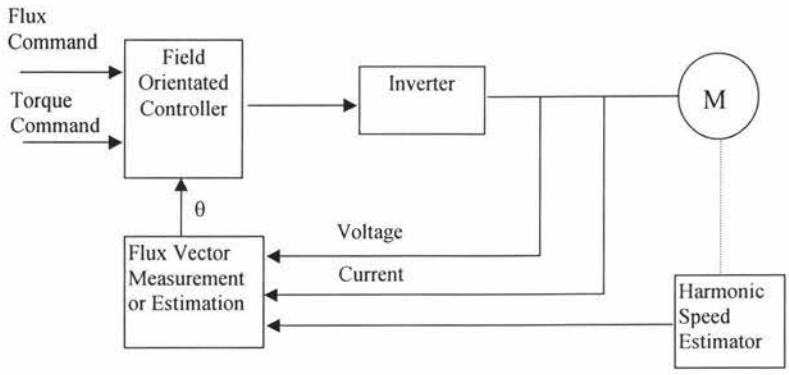

Figure 7.1 Direct Field Orientated System

REFERENCES

1. Donald S. Zinger, Francesco Profumo, Thomas A. Lipo, and Donald W. Novotny, "A Direct Field Orientated Controller for Induction Motor Drives Using Tapped Stator Windings", IEEE Trans. Power Electron., Vol. 5, No. 4, pp. 446-453, Oct. 1990.

2. J.Jiang, and J. Holtz, "High Dynamic Speed Sensorless AC Drive with On-Line Parameter Tuning and Steady State Accuracy", IEEE Trans. Industrial Elec., Vol. 44, No. 2, pp. 240-246, Mar./Apr. 1997.

3. Muneaki Ishida, and Koji Iwata, "A New Slip Frequency Detector of an Induction Motor Utilizing Rotor Slot Harmonics", Industry App., Vol. 20, No. 3, pp. 575-581, May/June 1988.

4. B. Hammerli, R. Tanner and R. Zwicky, "A Rotor Speed Detector for Induction Machines Utilizing Rotor Slots Harmonics and an Active Three-Phase Injection", 2nd European Conference on Power Electronics and Applications, pp. 599-604, 1987.

5. M. Hilairet, and F. Auger, "Frequency Estimation for Sensorless Control of Induction Motors", IEEE International Conference on Acoustics, Speech and Signal Processing, pp. 925-928, 2001.

6. Kevin D. Hurst, and Thomas G. Habetler, "Sensorless Speed Measurement Using Current Harmonic Spectral Estimation in Induction Machine Drives", IEEE Trans., pp. 601-607, 1996.

7. Nikolas Teske, Greg M. Asher, Mark Sumner, and Keith J. Bradley, "Encoderless Position Control of Induction Machines", Proc. EPE Conference Graz Austria Aug. 2001.

8. Jung-Ik Ha, and Seung-Ki Sul, "Sensorless Field-Orientation Control of an Induction Machine by High-Frequency Signal Injection", IEEE Trans. Industry App., Vol. 35, No.1, pp. 933-938, Jan./Feb. 1999.

9. Li Zhen, and Longya Xu, "Sensorless Field Orientation Control of Induction Machines Based on a Mutual MRAS Scheme", IEEE Trans. On Industrial Elec. Vol. 45, No. 5, pp. 45-51, Oct. 1998.

10. Young An Kwon, and Dae Won Jin, "A Novel MRAS Based Speed Sensorless Control of Induction Motor", IEEE Industrial Electronics Society 25 Conference, pp. 933-938, 1999.

11. Jehudi Maes, and Jan Melkebeek, "Speed Sensorless Direct Torque Control of Induction Motors using an Adaptive Flux Observer", Conference Record of IEEE Industry Appl. Conference 34th Annual Meeting , pp. 2305-2312, Oct. 1999.

12. Feri Yusivar, Kenji Uchida, Hiroyuki Haratsu, Shinji Wakao, and Takashi Onuki, "Speed Adaptive Observer for Sensorless IM Drive using Combined Reference Frames", APEC conference, pp. 127-132, Feb. 2000.

13. Francesco Parasiliti, Roberto Petrella, and Marco Tursini, "Adaptive Sliding Mode Observer for Speed Sensorless Control of Induction Motors", Conference Record of IEEE Industry Appl. Conference 34th Annual Meeting, pp. 2277-2283, Oct. 1999.

14. G. Garcia, E. Mendes, and A. Razek, "Reduced-order Observers for Rotor Flux, Rotor Resistance and Speed Estimation for Vector Controlled Induction Motor Drives using the Extended Kalman Filter Technique", IEEE Proc-Electr. Power App., Vol. 146, No. 3, pp. 282-288, May 1999.

15. Bharadwaj R. M., Parlos A.G., Toliyat H.A., "Adaptive Neural Network-Based State Filter for Induction Motor Speed Estimation", IEEE Industrial Society 25 Conference, pp. 1283-1288, 1999.

16. Subhasis Nandi, and Hamid Toliyat, "Detection of Rotor Slot and other Eccentricity Related Harmonics in a Three Phase Induction Motor with Different Rotor Cages", IEEE Trans. Energy Conversion, Vol. 16, No. 3, pp. 253-259, 2001.

17. Fang-Zheng Peng, and Tadashi Fukao, "Robust Speed Identification for Speed-Sensorless Vector Control of Induction Motors", IEEE Trans. Industrial Applications, Vol. 30, No. 5, pp. 1234-1240, 1994.

18. C. Ilas, A. Bettini, L. Feraris, G. Griva, and F. Profumo, "Comparison of Different Schemes Without Shaft Sensors for Field Orientated Control Drives", IEEE IECON, pp. 1579-1588, 1994.

19. L. B. Brahim, and R. Kurosawa, "Identification of Induction Motor Speed Using Neural Networks", IEEE PCC, Yokohama, pp. 689-694, 1993.

APPENDIX A

Table 1 0% load

Freq (Hz)	Current (A)	Speed (rpm)
77	0.45	500
70	0.45	450
62	0.45	400
53	0.45	350
47	0.45	300
39	0.45	250
32	0.45	200
24	0.43	150
18	0.41	100
13	0.38	50

Table 2 10% load

Freq (Hz)	Current (A)	Speed (rpm)
81	0.49	500
74	0.48	450
66	0.48	400
59	0.48	350
50	0.46	300
44	0.46	250
37	0.45	200
30	0.45	150
26	0.45	100
25	0.45	50

Table 3 30% load

Freq (Hz)	Current (A)	Speed (rpm)
88	0.55	500
78	0.54	450
71	0.53	400
63	0.53	350
56	0.51	300
48	0.49	250
42	0.49	200
36	0.49	150
32	0.49	100
28	0.48	50

Table 4 50% load

Freq (Hz)	Current (A)	Speed (rpm)
90	0.61	500
84	0.6	450
77	0.59	400
68	0.57	350
60	0.55	300
53	0.54	250
47	0.53	200
40	0.52	150
35	0.51	100
29	0.49	50

Table 5 60% load

Freq (Hz)	Current (A)	Speed (rpm)
105	0.76	500
96	0.73	450
88	0.71	400
78	0.67	350
69	0.64	300
63	0.63	250
55	0.6	200
46	0.57	150
40	0.54	100
32	0.51	50

Table 6 70% load

Freq (Hz)	Current (A)	Speed (rpm)
109	0.8	500
100	0.77	450
92	0.74	400
81	0.7	350
74	0.67	300
66	0.64	250
58	0.61	200
49	0.58	150
42	0.55	100
32	0.5	50

Table 7 80% load

Freq (Hz)	Current (A)	Speed (rpm)
116	0.87	500
107	0.83	450
98	0.79	400
88	0.75	350
79	0.71	300
69	0.67	250
61	0.63	200
53	0.59	150
44	0.55	100
35	0.5	50

Table 8 100% load

Freq (Hz)	Current (A)	Speed (rpm)
123	0.9	500
109	0.83	450
100	0.8	400
90	0.75	350
81	0.71	300
71	0.67	250
62	0.63	200
54	0.6	150
46	0.56	100
35	0.51	50

APPENDIX B

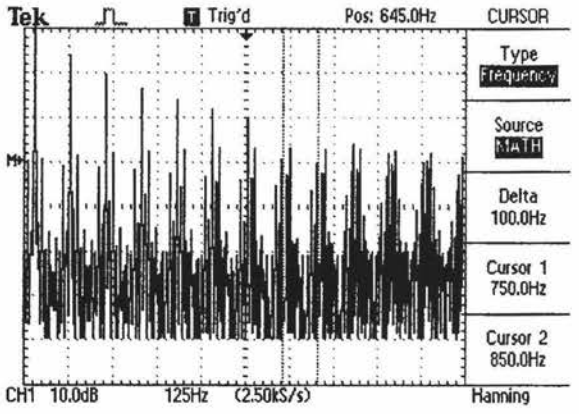

Figure 1 Harmonic Pairs at 1100rpm

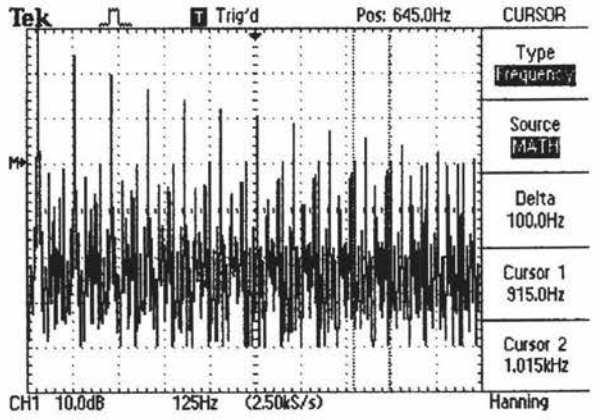

Figure 2 Harmonic Pairs at 1320rpm

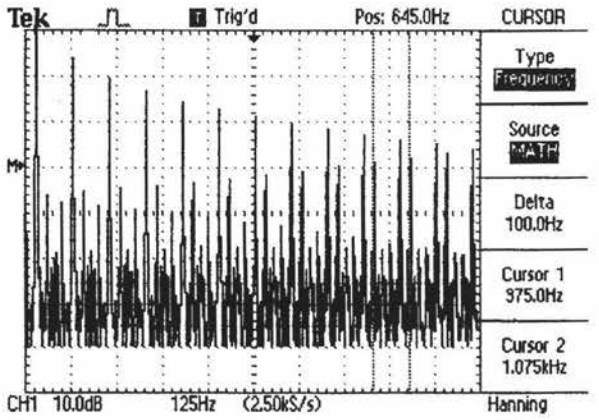

Figure 3 Harmonic Pairs at 1400rpm

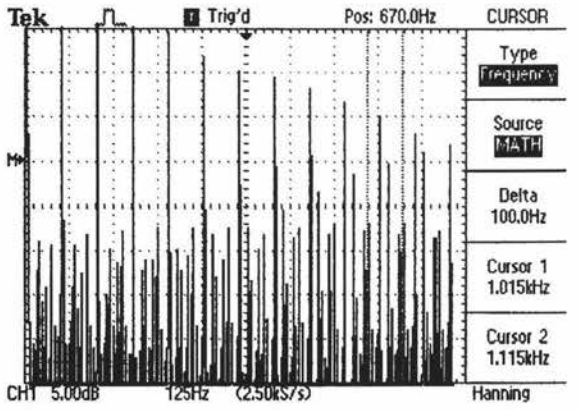

Figure 4 Harmonic Pairs at 1460rpm

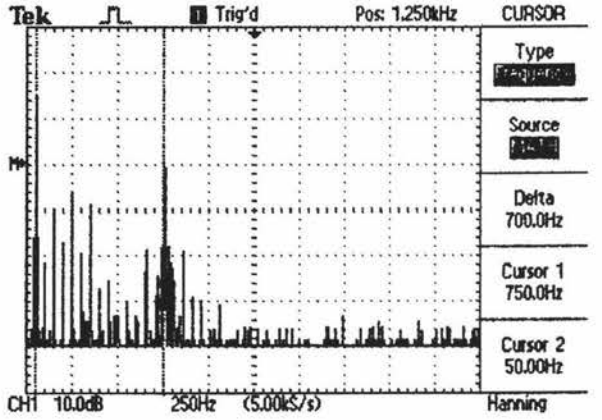

Figure 5 1st Order Filter Output at 1090rpm

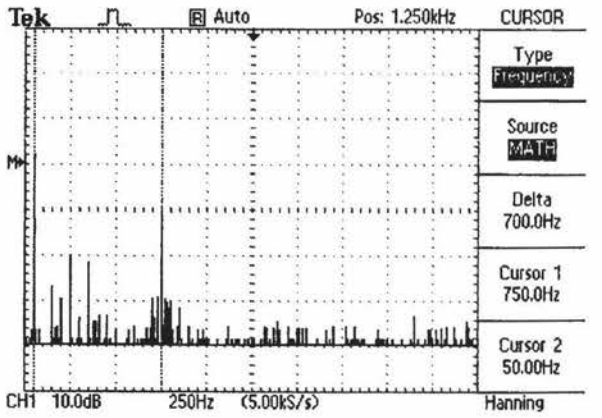

Figure 6 2nd Order Filter Output at 1090rpm

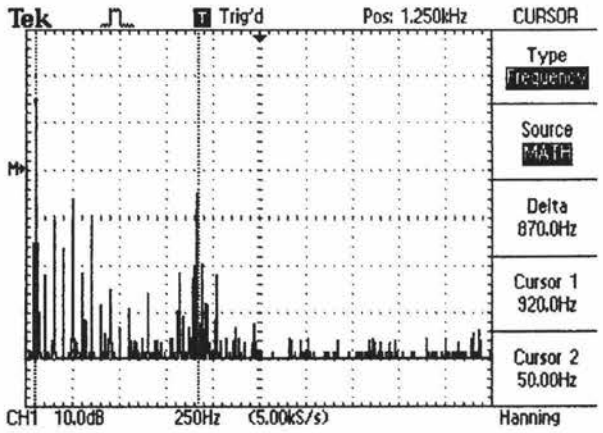

Figure 7 1st Order Filter Output at 1320rpm

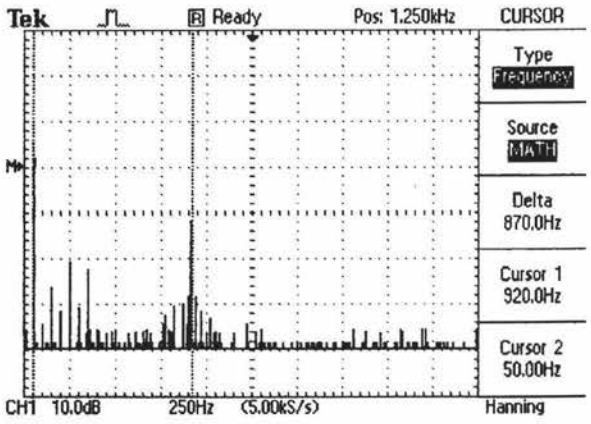

Figure 8 2nd Order Filter Output at 1320rpm

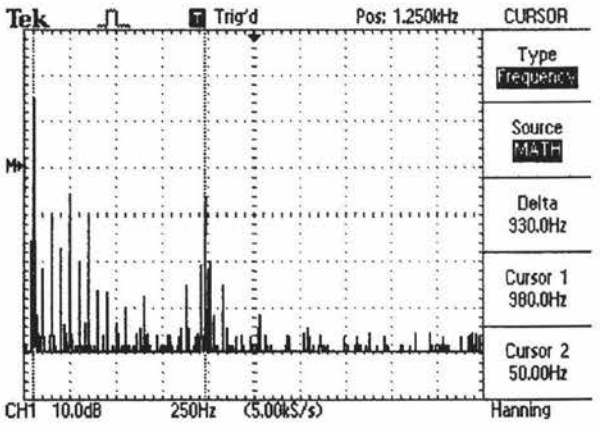

Figure 9 1st Order Filter Output at 1400rpm

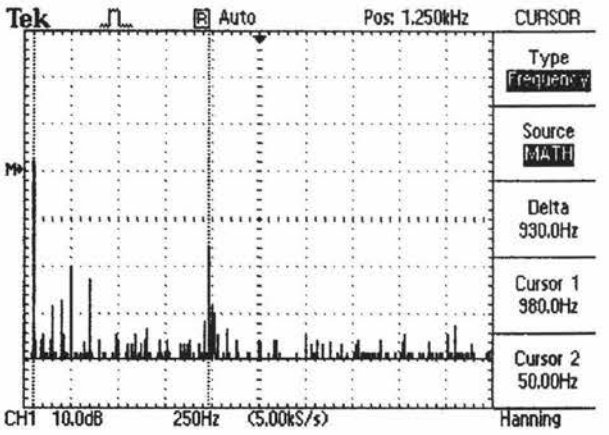

Figure 10 2nd Order Filter Output at 1400rpm

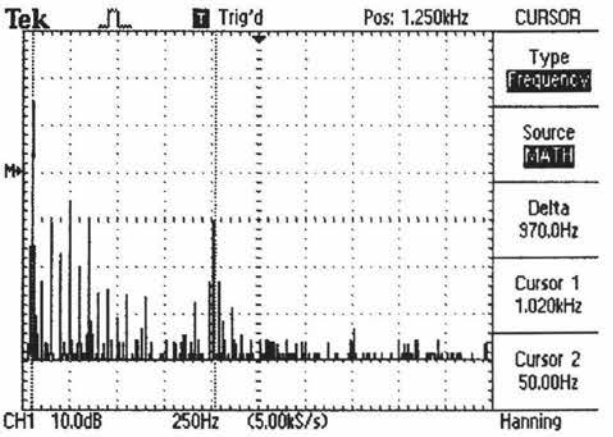

Figure 11 1st Order Filter Output at 1457rpm

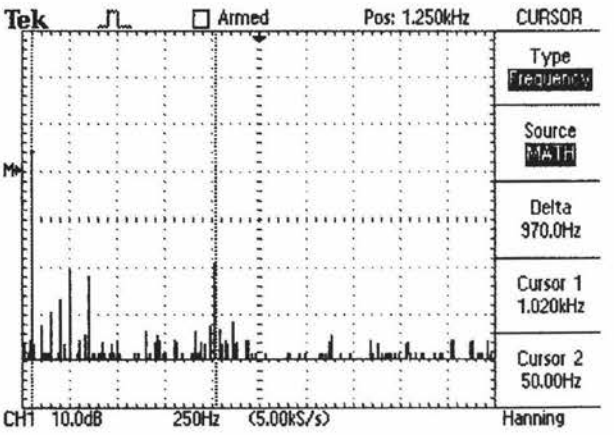

Figure 12 2nd Order Filter Output at 1457rpm

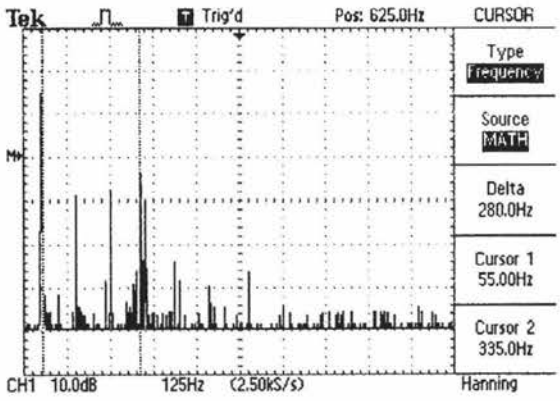

Figure 13 1st Order Filter Output at 520rpm

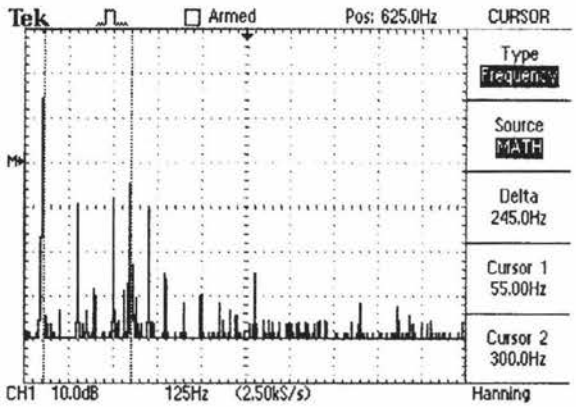

Figure 14 1st Order Filter Output at 470rpm

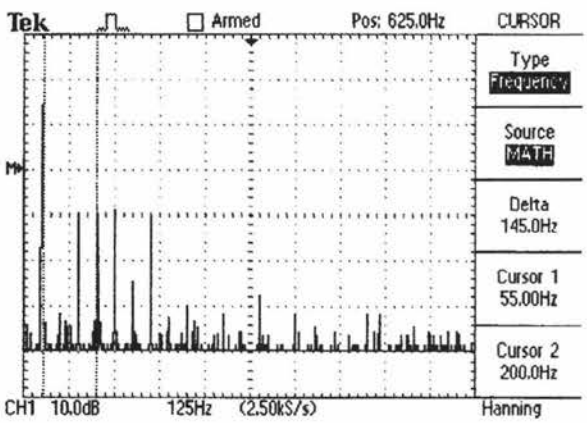

Figure 15 1st Order Filter Output at 340rpm